Magnetorotons in Quasi-Three-Dimensional Electron Systems

K. Karraï,[(1)] X. Ying,[(1)] H. D. Drew,[(1)] M. Santos,[(2)] M. Shayegan,[(2)] S.-R. E. Yang,[(3)] and A. H. MacDonald[(4)]

[(1)]*Joint Program for Advanced Materials, Department of Physics and Astronomy, University of Maryland, College Park, Maryland 20742 and Laboratory for Physical Sciences, College Park, Maryland 20740*

[(2)]*Department of Electrical Engineering, Princeton University, Princeton, New Jersey 08544*

[(3)]*Institute for Microstructural Sciences, National Research Council of Canada, Ottawa, Ontario, Canada K1A 0R6*

[(4)]*Department of Physics and Material Research Institute, Indiana University, Bloomington, Indiana 47405*

(Received 25 July 1991)

The dispersion relation for magnetoplasmons propagating perpendicular to the magnetic field is investigated for a quasi-three-dimensional electron system. The magnetic field is in the plane of a $\cong$100-nm-wide electron slab which is confined by a wide $Al_xGa_{1-x}As$ parabolic quantum well. A minimum is found in the magnetoplasma dispersion relation, indicating the existence of a magnetoroton excitation for wave vector q about twice the inverse magnetic length. Calculations of the dispersion relation within the single-mode approximation are in good qualitative agreement with the measurements.

PACS numbers: 71.45.Gm, 72.15.Nj, 73.20.Mf, 78.20.Ls

Strongly interacting electron systems are of great current interest. Examples range from the fractional quantum Hall effect (FQHE) in two-dimensional electron systems (2DES) to high-temperature superconductivity. Strong repulsive interactions frequently lead to the ground-state pair-correlation function becoming prominently peaked for particle separations near the mean interparticle spacing r_0. The Fourier transform $S(q)$ then tends to be prominently peaked at the corresponding wave vectors, $q \cong 1/r_0$. The collective excitation spectrum of such strongly correlated systems is generally expected to show minima at such wave vectors because of the possibility of making excitations which disturb the ground-state correlations only weakly. This connection is explicit when the excitation spectrum is approximated by using the single-mode approximation (SMA). One example is the FQHE where minima are expected [1] to occur in both the inter-Landau-level and the intra-Landau-level branches of the collective excitation spectrum close to the q where $S(q)$ is peaked. These minima are analogous to the roton minimum in the excitation spectrum of ^{4}He [1]. Direct measurement of the magnetoplasma dispersion relation in the FQHE state of a 2DES is difficult because of the need for a large-wave-vector [$q \cong 1/l_0$, where $l_0 = (\hbar/eB)^{1/2}$ is the magnetic length] low-energy probe [2]. Raman-scattering experiments [3] have been partially successful and, although they are not completely understood, can be interpreted as measuring a quantity proportional to the density of collective states. However, they give no information on the dependence of the collective excitation energy on q and hence provide only a very indirect probe of the ground-state correlations.

Three-dimensional electron systems also have prospects for novel ground states [4,5]. Hartree-Fock calculations show that various types of Wigner-crystal ground states may be possible [5]. Attempts to observe these states in bulk doped semiconductors have proven unsuccessful because the Coulomb interaction with the dopants leads to localization [6]. In remotely doped wide parabolic $Al_xGa_{1-x}As$ quantum wells grown by molecular-beam epitaxy (MBE), quasi-three-dimensional electron systems (Q3DES) have been realized [7–12]. These structures produce high-mobility nearly three-dimensional electron slabs (100 to 300 nm thick) with densities in the range of $5\times10^{15}/\mathrm{cm}^3$ to $5\times10^{16}/\mathrm{cm}^3$, that remain metallic in magnetic fields as high as 17 T at temperatures as low as 25 mK. The electron density is nearly constant over the thickness of the electron slab and its magnitude is determined by the curvature of the confining parabolic potential [7–12]. MBE-grown Q3DES have the unique advantage that potential modulations can be inserted in the potential profile which can permit the coupling of electromagnetic radiation to large-q excitations. Therefore these systems are good candidates for the observation of the dispersion relation for 3D magnetoplasmons. In this Letter we report the results of measurements of the energies of the collective excitations at large wave vectors in a Q3DES and the results are compared with the predictions of the SMA for a 3D electron system. This is the first measurement of the magnetoplasmon dispersion relation in a strongly interacting electron system.

The magneto-optical properties of Q3DES in wide parabolic quantum wells with **B** applied in the plane of the electron slab have been extensively studied [8–11]. In this geometry a single resonance is observed, independent of electron areal density N_s, at a frequency $\omega^+ = (\omega_c^2 + \omega_0^2)^{1/2}$, where ω_c is the cyclotron frequency and ω_0 is the harmonic-oscillator frequency characteristic of the parabolic well. Examples of the spectra observed for different N_s are shown in Fig. 1(a). When the electron slab is thick compared to l_0, this excitation is the plasma-shifted cyclotron resonance [8,9,11], and the plasma frequency $\omega_p = \omega_0$. It has been shown [9,11,13] that this is the only mode that couples to a homogeneous (i.e., $q=0$) electromagnetic field. It corresponds to the uni-

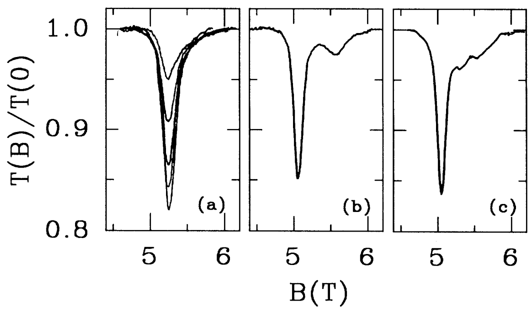

FIG. 1. Magnetotransmission spectra for three samples at 118.83-μm wavelength and $T=1.4$ K. (a) Sample with a pure parabolic profile shown for different N_s. W was changed from 20 to 100 nm. (b) Sample with positive δ planar periodic perturbations, 30-nm period. (c) Sample with a single δ planar perturbing potential at the center of the well.

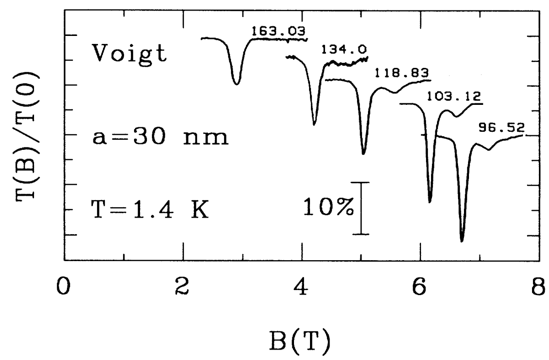

FIG. 2. Magnetotransmission spectra of a periodically perturbed parabolic well for different wavelengths. The numbers above the spectra indicate the infrared wavelength in μm. The spectra are displaced vertically for clarity.

form oscillation of the center of mass of the electron system at $\omega=\omega^+$ independent of N_s as observed in Fig. 1(a). This result [9] is known as the generalized Kohn theorem [13]. If the potential has deviations from parabolicity, it is possible to couple to the additional collective excitations of the Q3DES [11,12,14,15]. In order to study these nonuniform excitations of the Q3DES we have made measurements on quantum wells grown with controlled perturbing potentials superimposed on a parabolic potential.

We report measurements on five samples with similar 3D densities $n_0 \cong 2.5\times10^{16}$ cm^{-3} ($\omega_0 \cong 50$ cm^{-1}). Sample 1 is a pure parabolic well. The next two samples were grown with perturbations of period $a=20$ nm. Sample 2 was grown with an array of *positive δ planar* potentials by superimposing 0.5-nm-thick layers of $Ga_{1-y}Al_yAs$ with $y=0.005$ on a 300-nm-wide $Ga_{1-x}Al_xAs$ parabolic well (the integrated strength for each $Ga_{1-y}Al_yAs$ layer is $I=+2.5$ meV nm). In sample 3 a GaAs layer is inserted every 20 nm into the parabolic Al profile. The inserted GaAs layers represent a periodic array of *negative δ planar* perturbations for the electrons in the conduction band. The widths of the GaAs layers are adjusted so that each of these δ planar perturbations has an integrated strength of $I=-5$ meV nm. The fourth sample was grown with $a=30$ nm and a periodic array of δ planar perturbations with $I=+2.5$ meV nm. Sample 5 has a single δ potential $I=+7.5$ meV nm at the center of the well. In all samples the thicknesses of the in-plane perturbations are kept small compared to $l_0 \cong 10$ nm. The Al concentration profile of these samples was characterized by secondary ion mass spectroscopy, which permits a measurement of the thickness of the wide parabolic well, and, therefore, the period a.

Magnetoplasma excitations were measured in the quantum limit (i.e., only one spin-degenerate Landau level is occupied) with a magnetic field **B** (0–9 T) applied in the plane of the electron slab [9,11]. The electromagnetic radiation propagates perpendicular to the electron slab (Voigt geometry). The far-infrared radiation, which was generated by an optically pumped molecular-gas laser, was guided to the sample by light pipe optics, and was linearly polarized a few millimeters before the sample. The samples were immersed in liquid helium at 1.4 K. The transmitted light was detected using a composite Ge bolometer located outside the magnetic field at 4.2 K. The sample substrate was wedged 3° in order to avoid line-shape distortion due to interference effects. The spectra were measured by sweeping **B** at fixed laser frequencies. During the measurements it was possible to reduce N_s persistently using a red light emitting diode placed near the sample [10]. N_s, which was measured from the oscillator strength of the resonances, ranges typically from 10^{10}/cm^2 to 2.5×10^{11}/cm^2 [9]. At the largest electron densities, the effective thickness of the electron slab, defined as $W=N_s/n_0$, is $W \simeq 100$ nm, where n_0 is the 3D electron density determined optically from ω_p [8,9,11].

Typical transmission spectra for the three kinds of samples are shown in Fig. 1. For the pure parabolic potential only the Kohn mode ($\omega=\omega^+$) is observed as discussed earlier. For samples with a periodic array of δ planar perturbations a clearly resolved satellite resonance appears on the high-field side of the Kohn mode as seen in Fig. 1(b). It appears in the transmission spectra of the samples with positive as well as negative δ planar periodic perturbations. The relative strength of this satellite increases with **B** as seen in Fig. 2. The transmission spectrum of a well with a single perturbing δ potential in its center is shown in Fig. 1(c). In this case two satellites are observed. In all samples the resonances are observed only in the $\mathbf{E}\perp\mathbf{B}$ polarization. We show the N_s dependence of the spectra for the perturbed wells in Fig. 3. The amplitude of the satellite associated with the δ array is seen to increase rapidly with N_s as W grows and more δ potentials are covered by the electrons; however, its position remains independent of N_s. The satellites observed in the single δ samples are found to shift toward lower

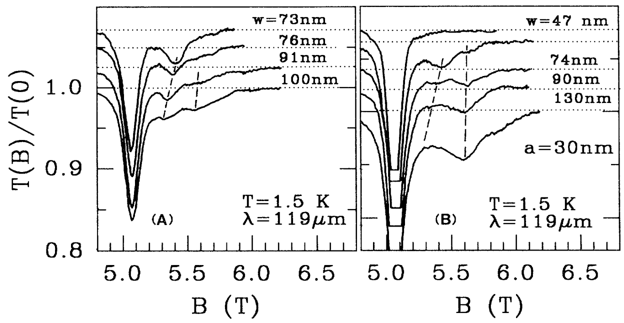

FIG. 3. Magnetotransmission spectra of a parabolic well with (a) a single δ planar potential perturbation, and (b) a periodic array of δ planar potential perturbations (30-nm period), for different N_s ($W = N_s/n_0$).

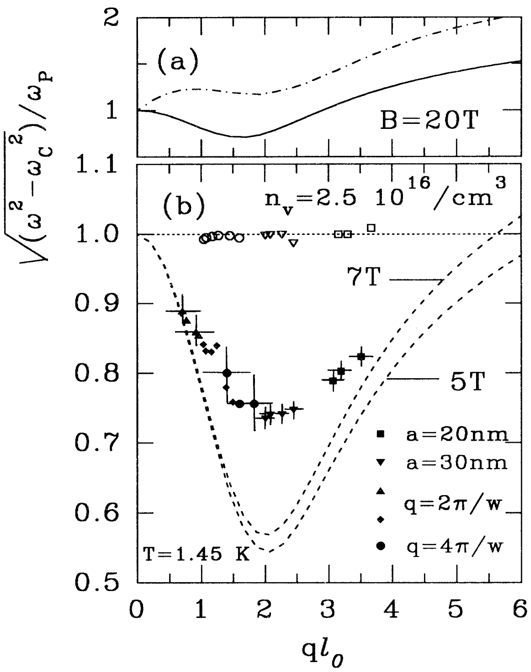

FIG. 4. Bottom panel: Normalized dispersion of the magnetoplasma modes. The dashed lines are the dispersion calculated in the SMA. Solid symbols correspond to the satellite modes and open symbols correspond to the Kohn mode plotted vertically above the satellite resonances. The minimum that appears at $ql_0 = 2$ is the "roton minimum." Top panel: Calculated magnetoplasmon dispersion curve at high field. Solid curve is for the Hartree-Fock fluid ground state. The dash-dotted curve is for a trial correlated ground state with lower total energy.

magnetic fields with increasing N_s [Fig. 3(a)].

We identify the distinct satellite resonance in the periodically perturbed samples as the magnetoplasma mode at $q = 2\pi/a$. The resonances observed in the single δ perturbed wells are identified as dimensional modes. Since the electron slab has a finite effective width W, standing magnetoplasma waves [12,15,16] (i.e., dimensional resonances) are expected to form along the normal of the electron system with $q = N\pi/W$ (for integer N). Since W increases with N_s, the q of these modes decreases with N_s. We also find evidence for dimensional modes in the periodically perturbed wells as can be seen in Fig. 3(b).

Coupling to the collective excitations of the Q3DES requires that the mode must have a nonzero dipole moment $p = \int \rho z\, dz$, where ρ is the charge fluctuation of the mode and z is normal to the slab [15]. In the ideal parabolic well, $p = 0$ for all modes except for the Kohn mode. For any symmetric confining potential only the odd modes can couple since $p = 0$ for the even modes. This immediately leads to the excitation of the dimensional modes with $q = N\pi/W$ ($N = 2,4,6,\ldots$) [17]. The periodic (symmetric) perturbation will also couple to other odd excitations which have the periodicity of the perturbation and which, in the infinite W limit, will reduce to standing magnetoplasmon modes at $q = 2\pi M/a$ (M an integer). The power absorbed by a mode is proportional to $E_z p$, where E_z is the ac electric field [18]. In the vicinity of the plasma-shifted cyclotron resonance, the radiation polarizes the electron slab along the growth axis z so that E_z is large. Therefore the coupling is strongest near $\omega = \omega^+$.

In order to reconstruct the magnetoplasma dispersion relation we have plotted the normalized satellite frequency $(\omega^2 - \omega_c^2)^{1/2}/\omega_p$ against the dimensionless wave vector $ql_0 = 2\pi l_0/a$ for the grating modes and $ql_0 = N\pi l_0/W$ for the dimensional resonances in Fig. 4(b). The corresponding data points are shown for 5 T $\leq B \leq$ 7 T. The measured position of the Kohn mode is also plotted similarly (open symbols) to demonstrate that it scales properly with magnetic field and to give an indication of the uncertainties in the resonance positions. The uncertainty in q for the dimensional resonances comes from the uncertainty in the measurement in N_s from the integrated oscillator strength of the absorption profile and is represented by the horizontal error bars. The resulting reconstructed magnetoplasmon dispersion relation shows the existence of a minimum excitation energy at $ql_0 \cong 2$—a roton minimum.

In order to relate these data to theory we have calculated the dispersion relation of 3D magnetoplasmons propagating perpendicular to the magnetic field. We have used the SMA in a way similar to that presented in Ref. [1]. The calculations were carried out using a Hartree-Fock ground state. The results are presented in Fig. 4(b) for two different magnetic fields. The pronounced minimum found at $ql_0 = 2$ can be understood in analogy with the theory of Ref. [1] as a roton minimum. Good qualitative agreement is found with the measured dispersion. There is discrepancy, however, in the mode frequency and this may be due to finite-size effects of the electron slab that are not included in the theoretical approach. In Fig. 5 we show the positions of both the Kohn mode and the dis-

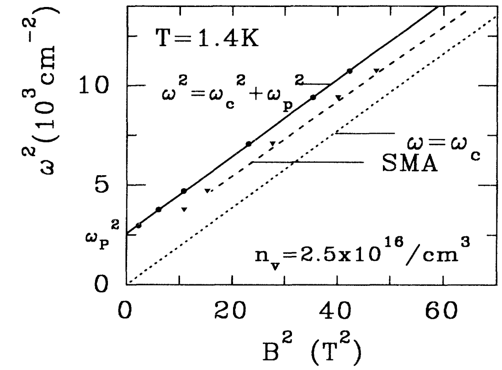

FIG. 5. ω^2 vs B^2 dependence of the plasma-shifted cyclotron resonance (circles) and of the satellite resonance (triangles) for sample 3. The dashed line is the calculated position of the magnetoplasma mode $\omega(q=2\pi/a)$, with $a=20$ nm and $\omega_p=51$ cm^{-1}. The dotted line is the cyclotron resonance.

tinct satellite mode of a periodic δ sample in a ω^2 vs B^2 plot. The calculated modes are also shown for $q=0$ and $q=2\pi/a$ ($a=20$ nm). In the SMA the magnetoplasmon dispersion depends only on the pair-correlation function in the ground state as expressed by $S(q)$. At stronger magnetic fields the Hartree-Fock ground state is crystalline [5]. However, studies [19] with trial wave functions with built in FQHE-like correlations demonstrate that strongly correlated fluid ground states, which differ qualitatively from the Hartree-Fock state, precede the Wigner-crystal state as the field strength is increased. In Fig. 4(a) we compare the SMA magnetoplasmon dispersion relations calculated from the Hartree-Fock fluid state with the dispersion relation calculated from a strongly correlated trial wave function [19]. The trial correlated state has a lower energy than the Hartree-Fock crystal [19] and the Hartree-Fock fluid state has the highest energy. The decrease in $\omega(q)$ at small q which occurs when the Hartree-Fock ground state is used reflects the decrease in the effective Coulomb depolarization potential when the wavelength of the collective mode becomes comparable to the quantized cyclotron orbit radius of the electrons. At large q the excitations are best regarded [1] as magnetoexcitons with particle-hole separation ql_0. The increase in $\omega(q)$ at large q reflects the loss of binding energy as electrons and holes are separated. The asymptote as q goes to infinity is the energy to make an unbound electron-hole pair. This energy is larger relative to the depolarization shift in more strongly correlated systems and this accounts for the difference in the shapes of the calculated $\omega(q)$ curves. The qualitative changes suggest that monitoring the magnetoplasmon dispersion can provide a signature of the strong correlations building in the system as the Wigner crystallization is approached.

Several aspects of these experiments remain to be clarified. The important question is the degree to which the 3D theory applies to the Q3D experiments. Indications that the 3D calculations may be adequate are found in calculations for a square well in zero magnetic field [20]. Also, a theory including the perturbations will be required to assess their effect on the mode frequencies and to understand their coupling to the radiation.

We would like to thank L. Brey, J. Dempsey, S. Das Sarma, H. Fertig, R. D. Grober, J. P. Kotthaus, and H. P. Wei for fruitful discussions. This work was supported by NSF Grants No. DMR-90-00553, No. DMR-89-21073, and No. DMR-88-02383.

[1] S. M. Girvin, A. H. MacDonald, and P. M. Platzman, Phys. Rev. B **33**, 2481 (1986), and references therein.

[2] S. Huant, G. Martinez, and B. Etienne, Europhys. Lett. **9**, 397 (1989), and references therein.

[3] A. Pinczuk, J. P. Valladares, D. Heinman, A. C. Gossard, J. H. English, C. W. Tu, L. N. Pfeiffer, and K. W. West, Phys. Rev. Lett. **61**, 2701 (1988).

[4] B. I. Halperin, Jpn. J. Appl. Phys. **26**, Suppl. 26-3, 1913 (1987).

[5] A. H. MacDonald and G. Bryant, Phys. Rev. Lett. **58**, 515 (1987), and references therein.

[6] M. Shayegan, V. J. Goldman, and H. D. Drew, Phys. Rev. B **38**, 5585 (1988).

[7] M. Shayegan, J. Jo, Y. W. Suen, M. Santos, and V. Goldman, Phys. Rev. Lett. **65**, 2916 (1990), and references therein.

[8] K. Karraï, H. D. Drew, M. W. Lee, and M. Shayegan, Phys. Rev. B **39**, 1426 (1989).

[9] K. Karraï, X. Ying, H. D. Drew, and M. Shayegan, Phys. Rev. B **40**, 12020 (1989); Surf. Sci. **229**, 515 (1990).

[10] K. Karraï, M. Stopa, X. Ying, H. D. Drew, S. Das Sarma, and M. Shayegan, Phys. Rev. B **42**, 9732 (1990).

[11] K. Karraï, X. Ying, H. D. Drew, M. Santos, and M. Shayegan, in *Proceedings of the Twentieth International Conference on the Physics of Semiconductors*, edited by E. M. Anastassakis and J. D. Joannopoulos (World Scientific, Singapore, 1990), p. 1278.

[12] A. Wixforth, M. Sundaram, K. Ensslin, J. H. English, and A. C. Gossard, Phys. Rev. B **43**, 10000 (1991).

[13] L. Brey, N. F. Johnson, and B. I. Halperin, Phys. Rev. B **40**, 10647 (1989).

[14] L. Brey, J. Dempsey, N. F. Johnson, and B. I. Halperin, Phys. Rev. B **42**, 1240 (1990).

[15] J. Dempsey and B. I. Halperin, Bull. Am. Phys. Soc. **3**, 1046 (1991).

[16] J. Alsmeier, E. Batke, and J. P. Kotthaus, Phys. Rev. B **40**, 12574 (1989); J. Alsmeier, J. P. Kotthaus, T. M. Klapwijk, and S. Bakker, Phys. Rev. B **39**, 2355 (1989).

[17] The power absorbed is $\mathcal{P}=\int J_z E_z\,dz$, where J_z is the current. From the continuity equation this leads to $\mathcal{P}\propto\int \rho z E_z\,dz \cong E_z p$ since E_z is nearly constant.

[18] C-V measurements show that the electron gas is nearly centered in the quantum well.

[19] S.-R. E. Yang, C. Gros, and A. H. MacDonald (to be published).

[20] W. G. Teich and G. Mahler, Phys. Status Solidi (b) **138**, 607 (1986).